Resilient Deformation Characteristics of Unsaturated Subgrade Materials of Rail Tracks under Cyclic Moving Wheel Loads

T. Ishikawa[1], B. Dareeju[2], C. Gallage[3], and L. Tianshu[1]
[1]*Faculty of Engineering, Hokkaido University, Sapporo, Japan*
[2]*Knight Piésold Consulting, Brisbane, Australia*
[3]*Science and Engineering Faculty, Queensland University of Technology (QUT), Brisbane, Australia*
E-mail: t-ishika@eng.hokudai.ac.jp

ABSTRACT: Water content of rail track subgrade materials fluctuates throughout the year due to the number of wetting and drying cycles, introducing unsaturated properties into the subgrade. Conservative rail track design guidelines are, however, mainly based on two extreme saturation conditions: fully dried or fully saturated. Current knowledge on the effects of subgrade water content on residual and resilient behaviour of the track foundation under the effects of Principal Stress Axis Rotation (PSAR) is limited and the potential of expansibility of foundation materials further upsurge the complexities towards the designing of the rail tracks. This study demonstrates the contributions of the PSAR on the resilient behaviour of foundation materials. Three different materials, including an expansive soil type have been subjected to drained cyclic vertical and torsional shear tests in a Modified Multi-Ring Shear (MMRS) apparatus and it is concluded that the resilient behaviour of the foundation materials is functions of the PSAR, material type, water content, and potential of expansibility.

KEYWORDS: Unsaturated foundation materials, Principal stress axis rotation, Resilient behavior, Expansive potential.

1. INTRODUCTION

Rail track subgrade experiences complex and repeated loads within its lifetime compared to road pavements. For new rail tracks, the effects of repeated loadings must be accounted to estimate the life of the track foundation and the cost of its replacement/maintenance from time to time (Gräbe and Clayton, 2009). The common practice is, however, using cyclic triaxial testing results to count the repeated loading conditions, which is, however, unable to replicate the moving wheel loading conditions due to the absence in the PSAR (Burrow et al., 2007; Gallage et al., 2013; Indraratna et al., 2017). Changing stress state of a soil element with the location of the train wheel is to be known as the PSAR (Lekarp et al., 2000) and its impacts on both residual and resilient deformation characteristics have been examined in the numerous conditions by laboratory element tests, model tests, field investigations and numerical modelling (Gai et al., 2018; Gräbe and Clayton, 2009; Ishikawa and Miura, 2015; Ishikawa et al., 2011; Yang et al., 2009, Hirakawa et al., 2002; Momoya et al., 2005). Two highly conservative ground conditions: fully dried/air-dried and fully saturated, have been, mainly, adopted in these studies.

The subgrade of a rail track, however, exhibits extremely complex saturation levels by the seasonal variations of groundwater level, inhabited activities, and climate change. Kodikara (2012) argued that own wetting and drying cycles within the season variations of unsaturated soil can be collapsed. Matric suction of the unsaturated subgrade materials mainly controls shear strength, which is a function of mechanical properties, particle size distribution, soil type, soil fabric orientation, and drainage boundary conditions (Bishop, 1959; Li et al., 2015; Salour et al., 2014; Han and Vanapalli, 2016). The matric suction is highly correlated with the soil water content, which is to be sensitive the climate changes (Rajeev et al., 2012). Understanding the effects of soil water characteristics on the track degradation process under repeated loading conditions is still associated with several uncertainties and is not considered in the rail track design even without the effects of the PSAR (Dareeju et al., 2014).

Furthermore, the track degradation process under repeated loading conditions is normally accounted into the design of rail tracks, using the resilient modulus. The resilient modulus of the subgrade is one of the key material properties required for the design of multi-layered flexible systems. Burrow et al. (2007) have further concluded that the resilient modulus is one of the key design criteria in conjunction with axle load, speed, and cumulative tonnage after comparing five different rail track foundation design guidelines. The resilient characteristics become predominant when the applied load is significantly lower than the shear capacity of soil and at the time, the residual deformation becomes negligible compared to the resilient component. However, the consequences of the resilient characteristics of either rail or road subgrades have been examined using cyclic/repeated single point/area loading conditions such as repeated load triaxial (RLT) or repeated load CBR (RLC) tests, where the PSAR cannot be implemented.

Furthermore, the resilient behaviour of soil depends on the stress state and soil characteristics such as type, the degree of saturation, the degree of compaction, and soil structure (Lekarp et al., 2000). Since the resilient modulus of soils tends to decrease with the saturation level of soil, the mechanistic design methods require the specifications to maintain both laboratory and corresponding field conditions under constant relative compaction and saturation levels. However, compared to the non-expansive soils, the expansive soils are subjected to a significant change of volume (swelling and shrinkage) due to changes in the saturation level, resulting in fluctuations in the resilient behaviour of subgrade materials. The resilient performance of both non-expansive and expansive unsaturated soils is well-established without accounting for the effects of the PSAR and this study is therefore experimentally investigated the effects of the PSAR of the non-expansive and expansive soils on the resilient performance of unsaturated rail tracks subgrade using a series of cyclic single point load (CSP), and cyclic moving wheel load (CMW) testing conditions.

2. TEST APPARATUS

Ishikawa et al. (2010) have developed a 'multi-ring shear apparatus', a type of torsional simple shear apparatus to examine the mechanical behaviour of coarse-grained materials of rail tracks subjected to repeated train passages. Inam et al. (2012) further evaluated the deformation characteristics of unsaturated road base course under the CMWL using the multi-ring shear apparatus. Addressing the limitations of the apparatus, Dareeju et al. (2017) modified the apparatus to examine the fine-grained materials and the performance of 'modified multi-ring shear (MMRS) apparatus to replicate the actual stress-strain state in rail track subgrade under the CMWL has been evaluated. Accounting for its ability to replicate the actual performance of the rail track subgrade, the MMRS apparatus, and its testing procedure have been adopted for this study.

Figure 1 illustrates the schematic diagram of the modified multi-ring shear apparatus. Hollow cylindrical specimens with 240 mm

outer diameter, 120 mm internal diameter, and 100 mm height are used in the MMRS tests. Detailed information of the MMRS apparatus and its incorporated modifications and its testing circumstances can be found in Dareeju et al. (2017). In the MMRS tests, the axial stress (σ_a) is calculated using the readings of the load cell located at the top of the loading plate. Axial strain (ε_a) is calculated from the vertical deformation measured by the external LVDT sitting on the top-loading plate. The radial strain (ε_r) and the circumferential strain (ε_θ) are zero in the MMRS specimens, the axial strain is a direct illustration of volumetric strain (ε_v). Both static and cyclic shear (torque) loadings are introduced through the direct drive motor placed under the bottom plate. The shear stress ($\tau_{a\theta}$) is calculated using torque transducer readings and the rotational angle of the direct-drive motor is used to calculate shear strain ($\gamma_{a\theta}$).

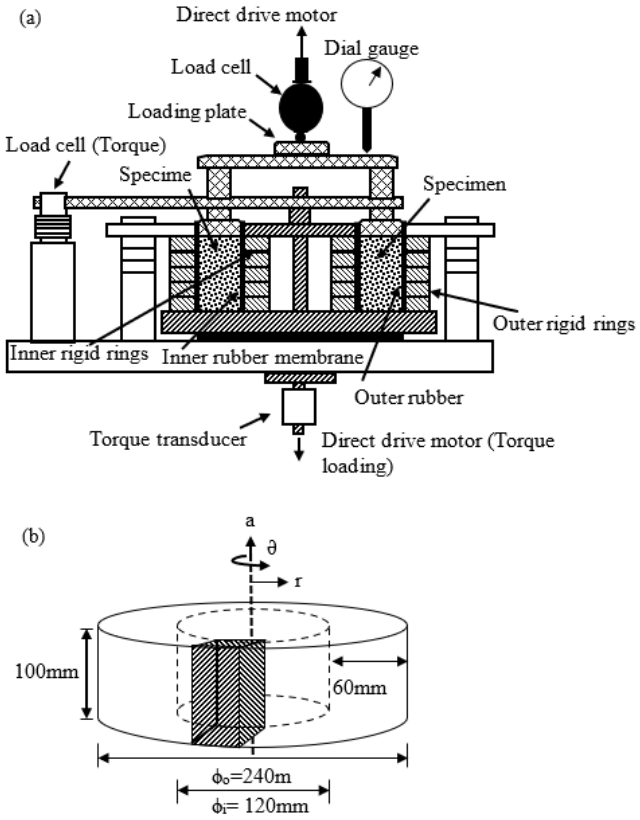

Figure 1 Modified Multi-Ring Shear (MMRS) apparatus: (a) schematic diagram and (b) soil specimen used (Dareeju et al., 2017)

3. TEST METHOD

3.1 Test Materials

Three different material types with two non-expansive soil types and one expansive soil type have been examined to replicate three different conditions as shown in Figure 2, which shows the particle size distributions of all soil types (i.e. Toyoura Sand, Type 'A' mixture, and Type 'B' mixture) used in this study, which were obtained from both wet sieving and hydrometer analyses under ASTM D6913/D6913M-17 (2017), and ASTM D7928-17 (2017) standard test methods, respectively. Table 1 summarises the basic properties of specific gravity, and particle sizes under the standard test method. According to Table 1, the maximum particle sizes of all materials used in this study are laid within standard specifications in sampling, where sample thickness is at least five times higher than the maximum particle size of the material. Toyoura sand can be classified as uniformly graded sand, while both soil mixtures as clayey sand according to the Unified Soil Classification system (USCS).

Table 1 Basic properties of materials used

Type	Specific Gravity	D_{max} (mm)	Coefficient of Uniformity
Type A	2.4	1.18	220
Type B	2.65	2.36	34
Toyoura Sand	2.65	2.36	1.59

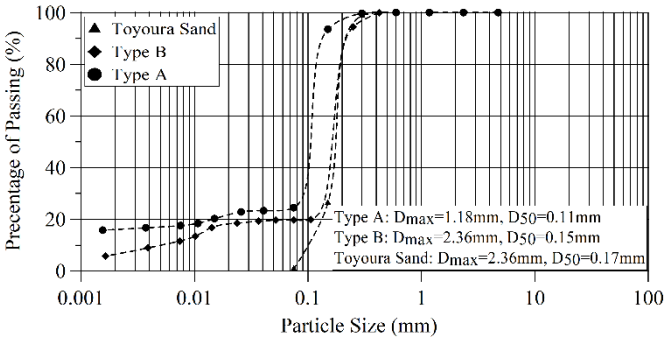

Figure 2 Particle size distribution of materials used

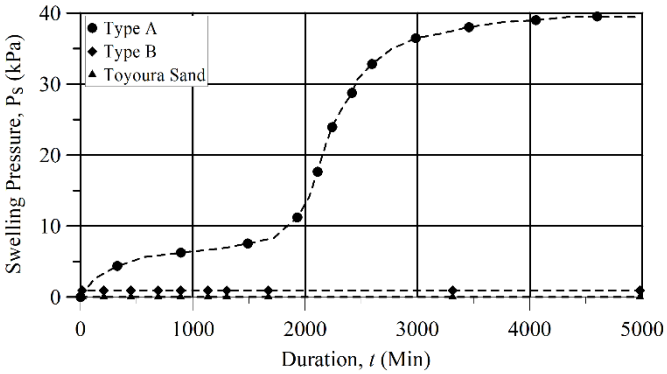

Figure 3 Swelling pressure of materials used

Type A sand-clay mixture was prepared by using 74.7% (total dry mass) of Silica sand and 25.3% of Bentonite, which has been developed to replicate Black Soil in Australia, considering the particle size distribution, Atterberg limits, and expansive properties. Black soil is a problematic weak expansive subgrade material for both rail tracks and roadways, especially in Australia and its performance at unsaturated state in road/rail subgrade is yet to be properly understood. Since Type A soil exhibits expansive properties, the Type B sand-clay mixture was designed with 80% of Toyoura sand and 20% of Kasaoka clay. Liquid limit and plastic limit of 104.8% and 27.7%, respectively were targeted in preparing soil mixtures to replicate the black soil behaviour. As shown in Figure 3, Type B soil does not indicate any expansive behaviour even having a similar particle size to Black soil/Type A soil. Figure 3 illustrates the swelling pressure of soil mixtures, which was measured using a constant rate strain (CRS) consolidation testing apparatus. Figure 4 shows the moisture-density relationships of the soil types obtained under the ASTM D1557 (2012) test method. The optimum water contents of Toyoura sand, Type A, and Type B are 14%, 12.8%, and 12.1%, respectively in correspondence with maximum dry densities of 1.62 g/cm^3, 1.57 g/cm^3, and 1.64 g/cm^3, respectively.

3.2 Sample Preparation

The soil water contents in preparing samples for this study were selected based on field observations and specimen water content uniformity of each material. Higher water content (degree of saturation) can, however, result in non-uniform specimens as the water of the MMRS specimen may penetrate to the lower part of the specimen during preparation and loading. Based on this limitation, the optimum water content of each material type was considered as the maximum water content for the MMRS tests. Considering the field observations and the non-uniformity of water content, four water

contents were selected for Toyoura sand as air-dried (Sr = 0.16%), 7.8% (Sr = 26%), 9.6% (Sr = 32%), and 14% (Sr = 47%). These water contents excluding air-dried are furthermore the corresponding water contents of MDD, 90% MDD, and 80% MDD of Toyoura sand, respectively. Compared to Toyoura sand, obtaining and maintaining targeted water contents in mixed soil samples was difficult due to their higher water absorption properties and it is difficult to achieve targeted dry density of specimen (95% MDD) using soils with higher water content due to the limitation of the MMRS apparatus. Only three water contents were therefore selected for Type A and Type B soil mixtures as shown in Table 2. After oven drying soil, water was added to achieve the pre-determined water contents. The soil was then kept in a controlled environment for 12 hours to the MMRS specimens were then prepared using three equal layers by tamping with a wooden hammer to achieve about 90% of the relative compaction of test materials. The sample was further compacted by applying vertical static loading on the sample under strain-controlled conditions with a constant rate of 0.1%/min to achieve the 95% of relative compaction of the test material. After sample preparation, the loading plate and associated system were set up to simulate static torsional shearing, cyclic single point loading, or cyclic moving wheel loading with precise loading conditions.

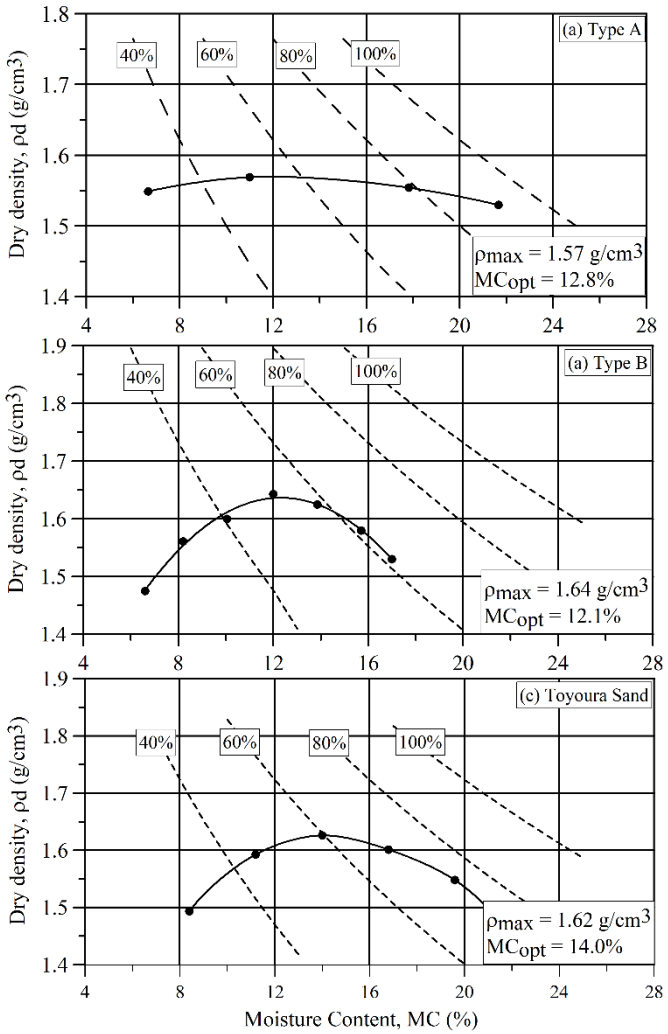

Figure 4 Density-moisture content relationships of materials used

Only consolidated drained (CD) test conditions were adopted in this study due to the limitation of the MMRS apparatus. Rail track subgrade is normally subjected to low-frequency loads, which have lower amplitude in a long distance. Under low-frequency loading conditions, the rail track subgrade experiences similar drainage conditions except under impact loads. Changes in water volume, soil suction, and pore-water pressure fluctuation of the MMRS specimens were unable to measure during the loading period. The change of gravimetric water content along the specimen height was therefore measured during different stages of the MMRS tests to confirm the uniformity of water content in the specimen as illustrated in Figure 5. Figure 5(a) illustrates the water content variations along with the sample height after the loading period with and without the effects of the PSAR and cyclic loading method does not significantly alter the water content distributions of the specimens according to Figure 5(a). As the MMRS specimens are not fully sealed at the top, sample drying within the loading period may be the key reason behind the fluctuation of water content distribution with sample height between after sample preparation and at the end of loading cycles as shown in Figure 5(b). To ensure the accuracy of this argument, the water content variations of specimens were observed after the loading period and after keeping the specimens without loading for a similar time of the loading. Considering the insignificant variations of water content during the loading period excluding the drying effects as shown in Figure 5(b), the methodology followed in this study can be considered as approximately suitable for investigating the influence of moving wheel loads on the plastic deformation characteristics of the unsaturated subgrade materials of rail tracks. Even the recent studies indicated that multiple states have different suction and degree of saturation at the same gravimetric water content, this study was unable to measure the variations in the degree of saturation and soil suction during sample preparation and loading conditions due to the limitations of the apparatus.

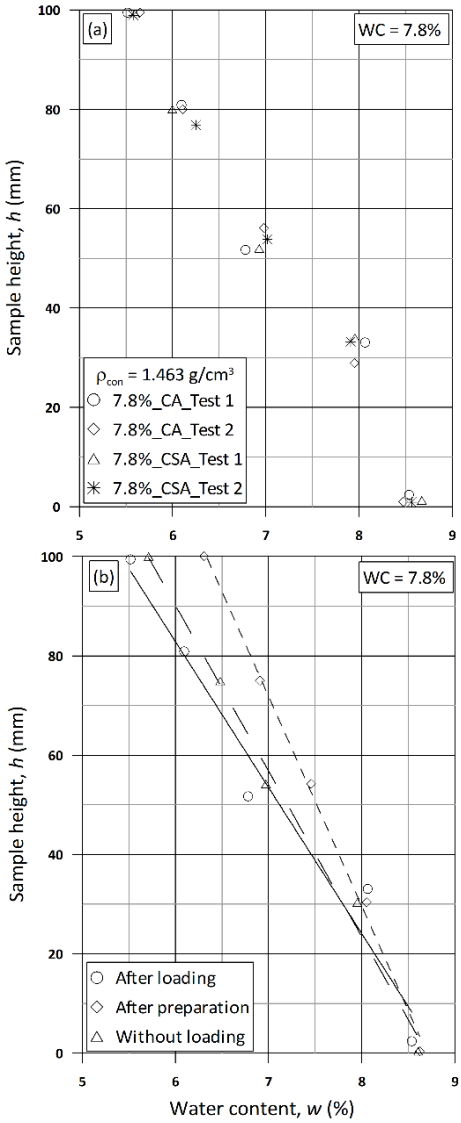

Figure 5 Water content distribution of sample along with the depth: (a) influence by loading and (b) influence during sample loading

3.3 Loading Conditions and Applications

Momoya (2004) performed a model test series to develop a relevant performance-based design method for rail track asphalt roadbed. Resilient and residual deformation characteristics of rail trackbed and subgrade were investigated using these experiment test results. The scale factor of 1/5 with the prototype was used to develop the model test. To evaluate the performance of the MMRS apparatus in accounting for the effects of PSAR on the cumulative plastic deformation of subgrade materials, these experimental results were used. Since axial load used in these model tests was only 1.5 kN, FEM analysis was performed to estimate actual stress state on the subgrade and resilient deformation characteristics by realistic train axle load. Two two-dimensional linear elastic FE models were developed by using ABAQUS finite element software (Hibbitt and Sorensen, 2005) since Momoya (2004) showed that three-dimensional FEM analysis did not make a significant influence on the actual stress state compared to 2-D FEM analysis due to plain stress conditions in the model tests. Figure 6 shows two-dimensional models developed for FEM analysis; a) Model 01 contains Toyoura sand as subgrade and bituminous stabilised crushed stone layer, and asphalt roadbed layer and b) Model 02 has Toyoura sand as subgrade and Ballast layer by replacing both bituminous stabilised crushed stone layer, and asphalt roadbed layer. The parameters used to develop the FE model can be found in Momoya (2004). In the FE model, the boundary condition of each side surface of the model was fixed for the direction perpendicular to the plane and free for the in-plane direction. Pinned with horizontal spring element was used as bottom boundary conditions to reduce the constraint since Momoya (2004) showed that horizontal spring element significantly influences on shear stress but no significant influence on vertical stress.

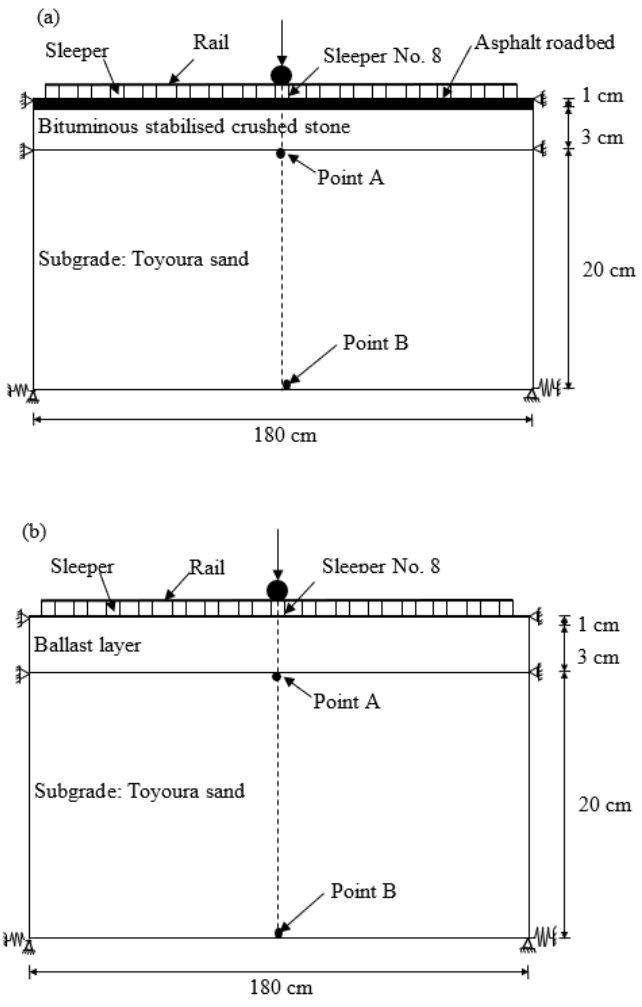

Figure 6 FE models: (a) Model 01 and (b) Model 2

Figure 7 shows the distributions of axial stress (σ_z) and shear stress (τ_{yz}) at the bottom of subgrade (Point B) obtained from both model test and FEM analysis (Model 01). There is a good agreement between the stress states of model tests and the FE model. This model is therefore used to obtain the actual stress state under real train axle loading conditions. Figure 8 illustrates the settlements of the track under the sleeper 8 with a moving wheel load of 1.5 kN with a speed of 600 mm/min from a small-scaled model test and FEM analysis (Model 01). According to Figure 8, the FE simulation agrees with the deformation characteristics measured from the small-scale model tests. In the small-scaled model test, the recovery process of displacement during unloading was lower than during loading because of the non-linear properties of rail track materials. In the FEM analysis, stiffness was however kept constant during both loading and unloading. This results in a similar displacement recovery process at both stages as given in Figure 8. A smaller plastic deformation appears at sleeper No. 8, after full loading cyclic in the small-scaled model test. Due to linear elastic material properties, this irreversible deformation is unable to replicate in FEM analysis. Following the validation of Model 01 using stress state at the bottom and track settlement, both bituminous stabilised crushed stone and asphalt roadbed layers were replaced in Model 01 by ballast layer to produce Model 02 as given in Figure 6(b).

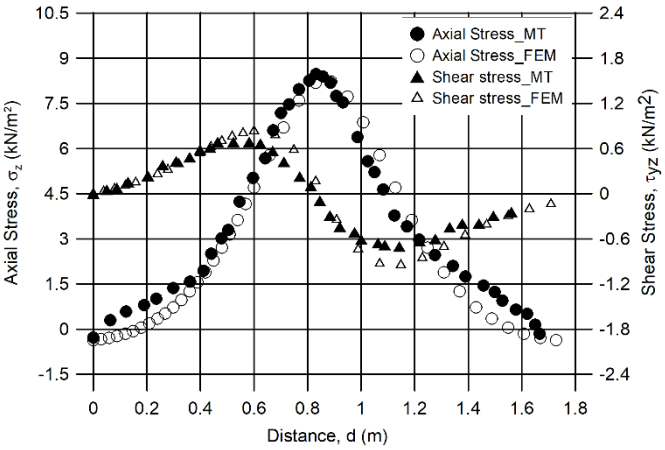

Figure 7 FE model validation with small scale model testing results for stress state (Model 1)

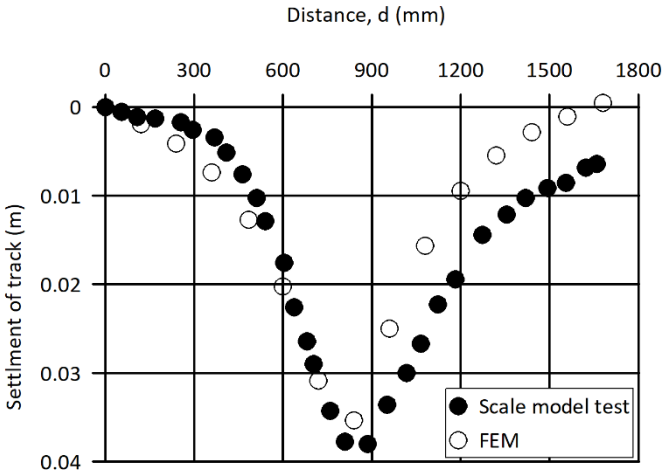

Figure 8 FE model validation with small scale model testing results for strain state (Model 1)

As a wheel load of 125 kN or an axle load of 25 tons is the most common axle load in rail track designing, Figure 9 shows the axial stress and shear stress distribution at point B under axle load of 125 kN in Model 01 and Model 02. According to Figure 9, asphalt roadbed in Model 01 can reduce both maximum axial and shear stresses at the bottom of subgrade by approximately 15% and 30%,

respectively compared to Model 02. Even asphalt roadbeds can reduce stress-strain characteristics of a rail track, Model 02 was selected for this study, as the typical approach is that using a ballast layer in rail track design for overcoming progressive shear failure and excessive plastic deformation of subgrade. Figure 10 illustrates the distributions of axial and shear stresses at the top of subgrade (Point A) in Model 02. Maximum axial stress and shear stress can be obtained from Figure 10 as 65 kN/m^2 and 18 kN/m^2, respectively. Adjacent two sleepers of each side of sleeper no. 8 introduce another two peaks in both axial stress and shear stress distributions as shown in Figure 10, however, the influence of these four peaks on cumulative residual deformation of the subgrade is neglected in this study due to the limitation of the MMRS apparatus. Only maximum axial stress and shear stress are used to develop loading conditions and two different experiment types; cyclic single point load test, and cyclic moving wheel load test were designed by using these maximum stress conditions to evaluate the effects of the water content of unsaturated subgrade on resilient characteristics under moving wheel loading conditions.

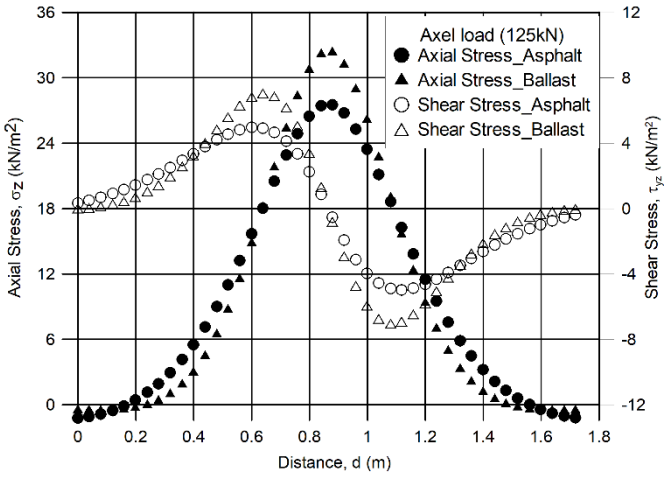

Figure 9 Stress state at bottom of subgrade (Point B) at sleeper No. 8 in FE models

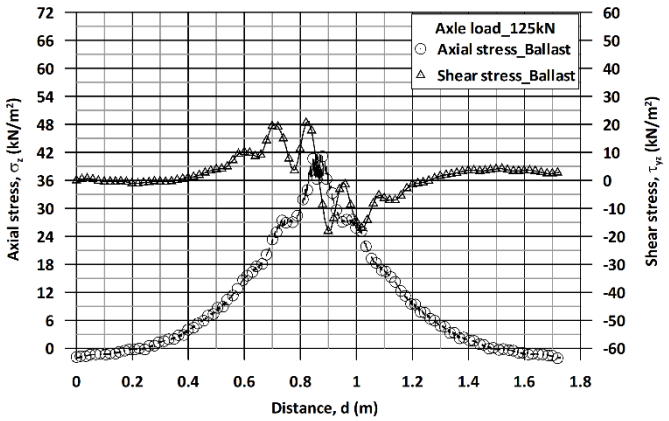

Figure 10 Stress state at top of subgrade (Point A) at sleeper No. 8 in FE models

Two types of different cyclic loading tests: cyclic single point load tests and cyclic moving wheel load tests, were performed to examine the effects of PSAR on the cumulative residual deformation of the unsaturated subgrade. To replicate cyclic triaxial loading conditions, cyclic single point load tests were performed, introducing axial stress in a half sinusoidal waveform with time and zero shear stress. The amplitude of axial stress of 65 kN/m^2 was achieved by 14 pre-loading cycles according to the conditions followed in model tests.

To replicate cyclic moving wheel load conditions, a series of cyclic axial and shear stresses loading tests were performed by introducing both axial stress in a half sinusoidal waveform and shear stress in sinusoidal waveform onto the MMRS specimen. Figure 11 illustrates the simplified loading waveforms developed using the results of FEM model results (i.e. Figure 10) to simulate the moving wheel loading conditions in the MMRS apparatus. The amplitude of both axial stress and shear stress was achieved by 14 pre-loading cycles, like cyclic single point load tests. Shear stress in cyclic moving wheel load tests was applied for bidirectional loadings, like two-way traffic on a rail track by changing the phase angle of shear stress by 180 degrees in every succeeding loading cycle. Table 2 illustrates all loading conditions adopted for this study. All cyclic MMRS tests were loaded for 200 loading cycles with 0.006 Hz loading frequency. The limitation of the MMRS apparatus and speed of the model tests were considered in defining the loading frequency. However, Inam et al. (2012) argued that lower frequency in cyclic loading provides enough time for plastic deformation in multi-ring shear tests. Additionally, Dareeju et al. (2017) indicated that the selection of the lower frequencies in the MMRS cyclic testings may cause underestimated deformation characteristics due to the absence of dynamic effects or amplification. Following a series of large-scale cyclic triaxial tests, Sun et al. (2015) indicated that increasing loading frequency and the number of loading cycles produces increased permanent deformation of ballast layers. A similar observation was documented by (Yang et al., 2009; Gräbe and Clayton, 2009), where higher loading frequency can generate higher plastic deformation with the presence of dynamic effects in subgrade materials and the dynamic effects become dominant after reaching the train speed to the speed of 10% of the Rayleigh wave speed (Yang et al., 2009). Table 2 summarises experimental conditions followed in cyclic single point load tests and cyclic moving wheel load tests.

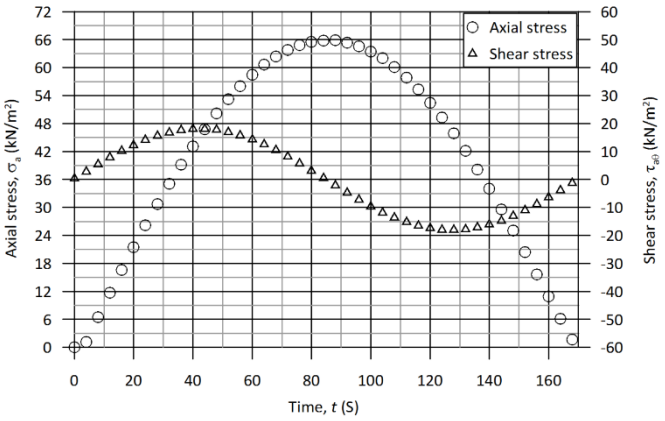

Figure 11 Stress states of cyclic moving wheel loading tests in MMRS apparatus

4. RESULTS AND DISCUSSION

The performance of the rail track subgrade under cyclic loading conditions critically controls the track degradation process, whereas the resilient capacity of the rail track is defined as a function of the resilient modulus in the rail track design guidelines. As the resilient behaviour is functions of loading state, soil type, and soil physical state, the stress state and its history have been maintained constant in this study, excluding the PSAR. Furthermore, loading frequency and relative compaction to be maintained constant, while the degree of saturation as a function of gravimetric water content and soil type have been changed following Table 2. Due to the limitations of the apparatus, the pore pressure response and radial stress have not been measured. However, Gräbe and Clayton (2014) observed a very slight change in the pore pressure in the saturated samples with higher fine percentages during the cyclic loading. The pore pressure response on the results of the tests in this study including Toyoura sand samples are negligible due to adopted CD testing conditions, unsaturated behaviour of materials, and the above observations.

Table 2 Experimental conditions adopted for the study

Cyclic Single Point Loading Tests							
Soil type	**Consolidated dry density, ρ_d (g/cm^3)**	**The ratio of OMC (%)**	**Axial Stress, σ_a (kPa)**	**Shear Stress, $\tau_{a\theta}$ (kPa)**	**Pre-loading cycles, N_{pc}**	**Loading cycles, N_c**	**Loading Frequency, *f* (Hz)**
Type A	1.493	0	65	0	14	200	0.006
	1.493	80	65	0	14	200	0.006
	1.493	90	65	0	14	200	0.006
Type B	1.561	8	65	0	14	200	0.006
	1.563	80	65	0	14	200	0.006
	1.563	90	65	0	14	200	0.006
Toyoura Sand	1.466	0	65	0	14	200	0.006
	1.467	55	65	0	14	200	0.006
	1.468	70	65	0	14	200	0.006
	1.465	100	65	0	14	200	0.006
Cyclic Moving Wheel Loading Tests							
Soil type	**Consolidated dry density, ρ_d (g/cm^3)**	**The ratio of OMC (%)**	**Axial Stress, σ_a (kPa)**	**Shear Stress, $\tau_{a\theta}$ (kPa)**	**Pre-loading cycles, N_{pc}**	**Loading cycles, N_c**	**Loading Frequency, *f* (Hz)**
Type A	1.493	0	65	18	14	200	0.006
	1.492	80	65	18	14	200	0.006
	1.490	90	65	18	14	200	0.006
Type B	1.560	8	65	18	14	200	0.006
	1.563	80	65	18	14	200	0.006
	1.568	90	65	18	14	200	0.006
Toyoura Sand	1.467	0	65	18	14	200	0.006
	1.466	55	65	18	14	200	0.006
	1.468	70	65	18	14	200	0.006
	1.468	100	65	18	14	200	0.006

4.1 Resilient Deformation Characteristics

The failure or rutting of the subgrade, which occurred by the permanent axial deformation is addressed in the design guidelines accounting for the resilient characteristics of subgrade materials. Figure 12 illustrates the cumulative maximum deformation of unsaturated specimens with and without the PSAR under different moisture contents. Dareeju et al. (2017) and Ishikawa et al. (2010) showed that maximum deformation of unsaturated materials is an indication of the resilient deformation by analysing the hysteresis loops of axial stress-axial strain relationships of cyclic loading tests. The difference between maximum axial strain during loading and minimum axial strain during unloading of each loading cycle, named strain amplitude gradually increases within early loading cycles and then, it approximately becomes a constant with increasing loading cycle number. A similar trend can be observed in Figure 12, where at early loading cycles, the maximum cumulative axial strain of all unsaturated specimens irrespective of the degree of saturation, soil type, and loading method, significantly increased illustrating early settlement at the early stage of the loadings. The settlement rate/degradation rate of the specimens gradually decreases with increasing loading cycle numbers introducing the resilient performance into the unsaturated specimens. A similar trend observes on the rail tracks, experiencing larger deformation during its early stages of the service life, and progressively stabilise the settlement. A similar trend has been observed by Dareeju et al. (2017), Gräbe and Clayton (2009, 2014), and Ishikawa et al. (2010).

The subgrade materials dominated over coarse-grained particles normally trend to considerably deformation under cyclic loading conditions compared to the fine-grained materials (Gräbe and Clayton, 2009, 2014). However, Toyoura sand has the lowest maximum cumulative axial strain compared to two fine-grained soil specimens irrespective of the loading conditions and degree of saturation as shown in Figure 12. The least compressibility of Toyoura sand, the consolidated drain testing conditions, and early settlement during pre-loading cycles as shown in Table 2 may be the possible reasons behind this lowest resilient deformation characteristics. Out of two fine-grain materials, non-expansive soil (Soil Type B) has been subjected to higher resilient deformation regardless of either loading condition or degree of saturation excluding air-dried conditions as shown in Figure 12. The swelling pressure of Type A material has lowered the deformation under cyclic loading conditions. This may therefore deceive considering higher resilient capacity in the design of the rail track compared to non-expansive soil. However, after diminishing the swelling potential of expansive or sensitive materials (i.e. at the end of free swelling), the expansive soil may trend to significantly deformation resulting in lower resilient capacity. Further studies however require examining the performance of expansive soil with minimum swelling potential under cyclic loading conditions.

4.2 Resilient Moduli of Unsaturated Subgrade Materials

The hysteretic stress-strain relationship during cyclic loading is fundamental to estimate the four different modulus parameters: equivalent (E_{eq}), tangential (E_{tan}), secant (E_{sec}), and maximum (E_{max}). Using the unloading curve of the hysteretic loop (i.e. strain amplitude), the equivalent resilient modulus of each unsaturated specimen subjected to different types of cyclic loadings has been estimated by Eq. (1). Figure 13 illustrates the calculated E_{eq} values of the drained cyclic loading of the materials. Even application of cumulative resilient deformation is common to evaluate the influence of cyclic loading on the strain hardening of the materials, this study has employed the strain amplitude of each hysteretic loop to estimate

the resilient modulus of unsaturated specimens. As explained in Figure 12, the strain amplitude is substantially ineffective compared to the plastic deformation, resulting in a larger resilient modulus at the early of the loading cycles. As eventually, the subgrade materials are capable of achieving the resilient properties (i.e. apparent elastic), the resilient modulus of material gradually decreases and becomes approximately constant irrespective of the experimental conditions. Furthermore, the lower resilient modulus has been estimated for all samples, which were subjected to the PSAR and a similar trend has been observed by Gräbe and Clayton (2014) on fully saturated fine-grain constituted materials.

$$E_{eq} = \frac{\sigma_a}{\varepsilon_{ar}} \quad (1)$$

where; σ_a: axial stress and ε_{ar}: strain amplitude

The E_{eq} of Type A, Type B, and Toyoura sand at 200 loading cycle varies between 23 – 84 MPa, 32 – 96 MPa, and 57 – 341 MPa, respectively as shown in Figure 13. The typical range of resilient modulus of subgrade material is 15 to 100 MPa (Sayeed, 2016). A field measured resilient modulus of compacted unsaturated subgrade and subbase material in South Africa has values ranging from 70 to 500 MPa (Gräbe et al., 2005). Furthermore, O'Riordan and Phear (2001) concluded that the lower limit of subgrade resilient modulus needs to be capped at 25 MPa to enhance the integrity of the rail track. All resilient modulus observed within this study excluding air-dried samples is higher than recommended lower limit and within the typical ranges of the resilient modulus. Therefore, it may be considered that the findings of this study are directly applicable to the rail industry.

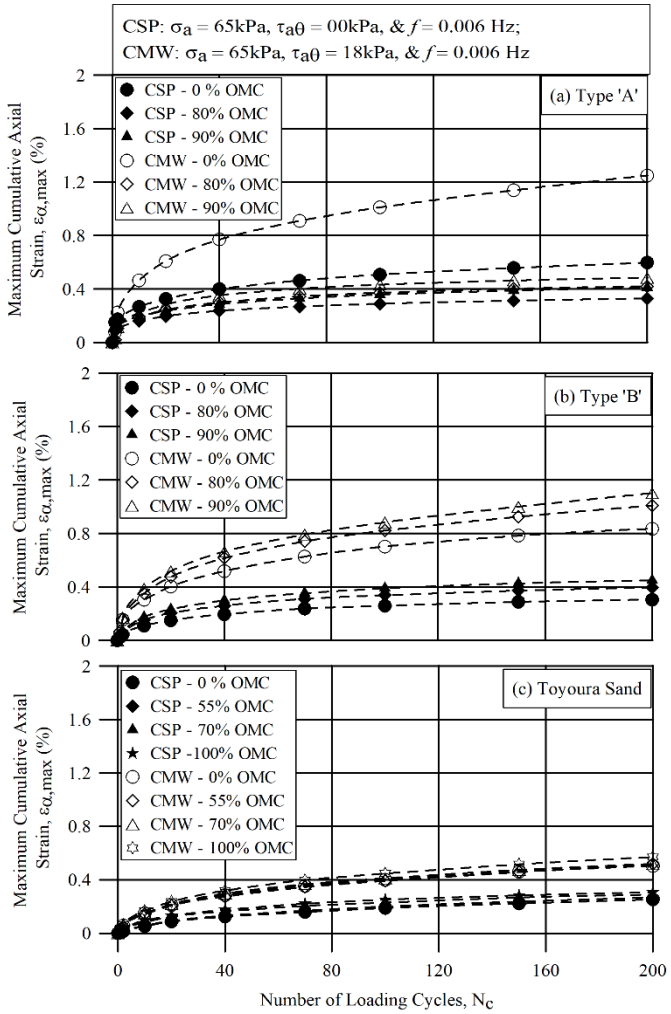

Figure 12 Maximum cumulative axial strain under cyclic loading conditions

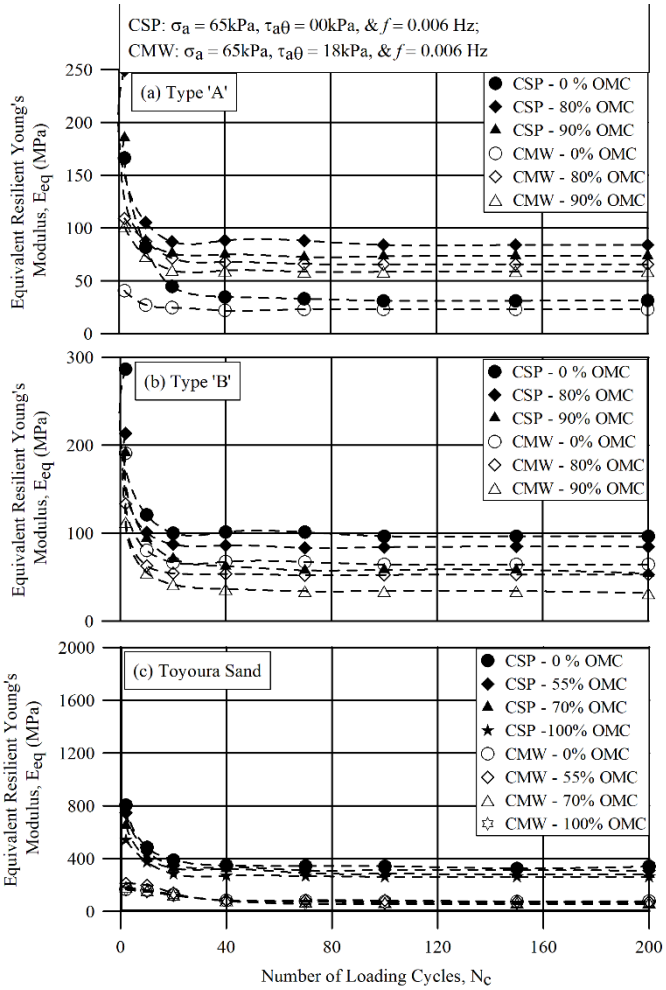

Figure 13 Resilient modulus of unsaturated subgrade materials

4.3 Effects of Moisture Content on Resilient Moduli

Figure 14 illustrates the relationships between the equivalent resilient modulus and moisture content of the materials examined in this study, where the moisture content and resilient modulus are presented as a ratio of optimum moisture content and at 200 loading cycles, respectively. The resilient modulus of Toyoura sand gradually decreases with an increasing degree of saturation irrespective of the loading conditions. This indicates that there be a larger accumulation of permanent deformation in coarse-grain subgrade materials at higher saturation levels. The reduction of inter-particle friction with the presence of water in Toyoura sand can be possible behind the declined resilient modulus with the saturation level.

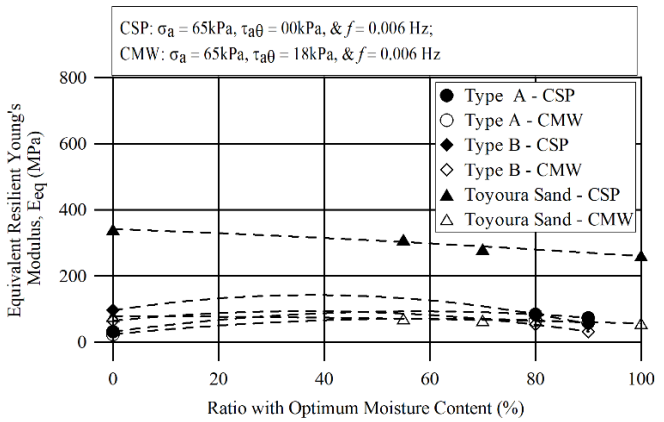

Figure 14 Effects of Saturation of Resilient Moduli

Normally, cohesion, matric suction, and water menisci are dominant in fine-grain materials. The presence of water in these materials can result in curved menisci at the particle contact point, resulting in normal force at the plane of contact. This circumstance enhances the resistance to compression under cyclic loads and a higher resilient modulus can be the consequence. However, the use of this apparent resilient modulus can significantly underestimate the performance of the rail track subgrade at the design stage. Though the soil Type B is a fine-grain material, it does not follow the common trend of the unsaturated material under cyclic loading conditions as shown in Figure 14. To draw a better conclusion on the resilient performance of Type B material, therefore, the range of saturation level requires to be extended.

Expansive Type A material illustrates the above-mentioned typical trend on fine-grain materials as given in Figure 14. Excluding the three dominants of fine material, the swelling potential can also control the compressibility of the material under cyclic loading conditions. When saturation level is negligible, the resilient modulus reduces due to the lower potential of swelling and higher air-void ratio. Increasing the saturation level boosts the swelling potential and lowers the compressibility.

4.4 Effects of Principal Stress Axis Rotation on Resilient Moduli

To quantify the degree to which the PSAR affected the performance of rail track subgrade, Ishikawa et al. (2010) has introduced 'ratio of axial strain' and Dareeju et al. (2017) further showed its applicability evaluating the performance of the MMRS apparatus. However, this parameter is predominantly defined to quantify the deformation characteristics, Gräbe and Clayton (2014) define the ratio of resilient modulus by dividing the resilient modulus without the PSAR by the resilient modulus with the PSAR as given in Eq. (2).

$$PSAR_{ratio} = \frac{E_{eq_{(without\ PSAR)}}}{E_{eq_{(with\ PSAR)}}} \quad (2)$$

At the early of the loading cycles, the ratio of resilient modulus decreases irrespective of the saturation level as shown in Figure 15, and eventually becomes constants. Generally, after approximately 40 loading cycles, the ratio does not impact by the loading cycle number under all experimental conditions. This indicates when the experimental conditions excluding the PSAR are constant, the impacts of the PSAR on the resilient performance of any subgrade materials can be predicted by the results of cyclic single-point loading tests such as repeated load triaxial or CBR.

There is an optimum ratio of optimum moisture content corresponding to the minimum ratio of the resilient modulus of all soil types as shown in Figure 16, which shows the relationships of the ratio of resilient modulus and moisture content at the 200 loading cycle. The effects of the PSAR on the resilient modulus are lesser at this ratio of optimum moisture content and use of the results of the cyclic single point loading tests at this moisture content can create lesser impacts compared to other saturation levels. Furthermore, the optimum ratio of OMC trends to be independent of the material types with exclusive of expansive soil types. The optimum ratio of OMC is approximately 40% for the non-expansive soil and the ratio of OMC gradually decreases with increasing saturation level as given in Figure 16. However, during the construction of subgrade or subbase (embankment), the moisture content of the materials is typically maintained at a range of ±5% (i.e. 95% to 105% OMC) of OMC in achieving the target dry density. Therefore, it is impractical to maintain 40% of OMC at the field throughout the compaction due to its higher requirement of energy to obtain target dry density. Consequently, the use of resilient modulus obtained from cyclic single point loadings at higher saturation levels underestimate the deformation characteristics of the subgrade materials, which results in frequent maintenance cycle within the service life of the rail track.

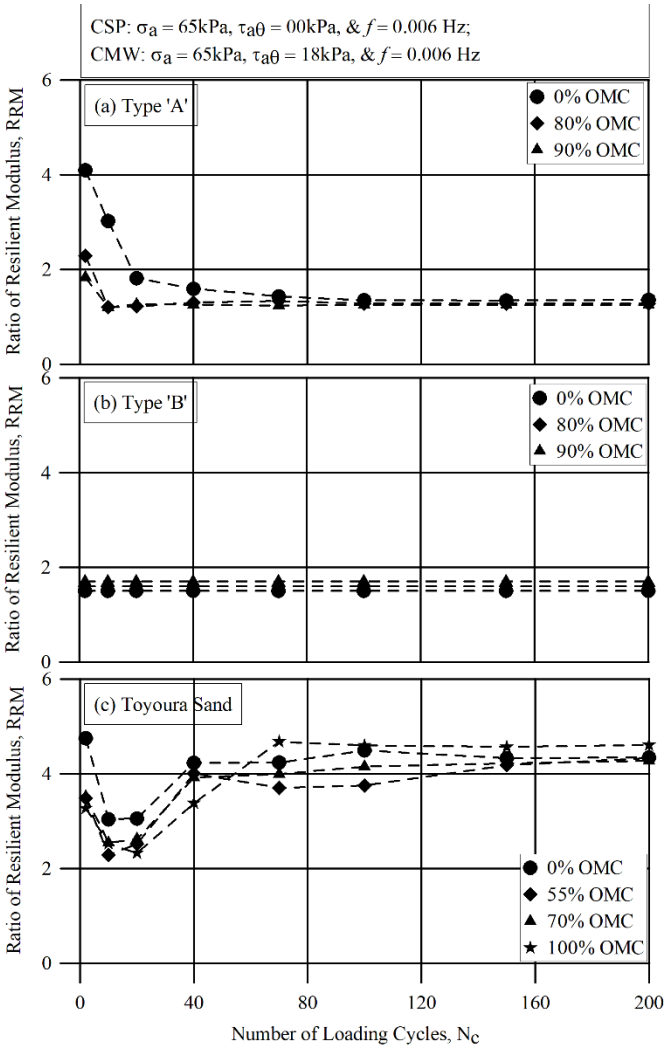

Figure 15 Ratio of resilient modulus of unsaturated specimens

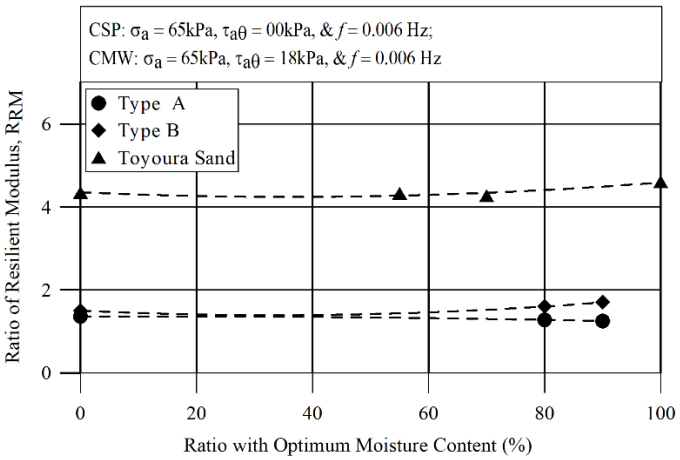

Figure 16 Effects of PSAR on resilient behaviour as a function of moisture content

To estimate the single amplitude of shear strain on the resilient modulus of the unsaturated subgrade materials, the single amplitude of shear strain has been estimated for each soil type at 200 loading cycle and illustrated as a function of the ratio of the resilient modulus as given in Figure 17. The results indicate that the ratio of resilient modulus increases with increasing the single amplitude of shear strain irrespective of the soil type. Ishikawa and Miura (2014) showed that residual deformation in cyclic moving wheel loading tests is mainly caused by the shear deformation of the specimen, where the compression is dominant in cyclic single-point loading conditions.

Similarly, it seems that the resilient modulus also depends on these two different mechanisms, which depend on the presence of the PSAR.

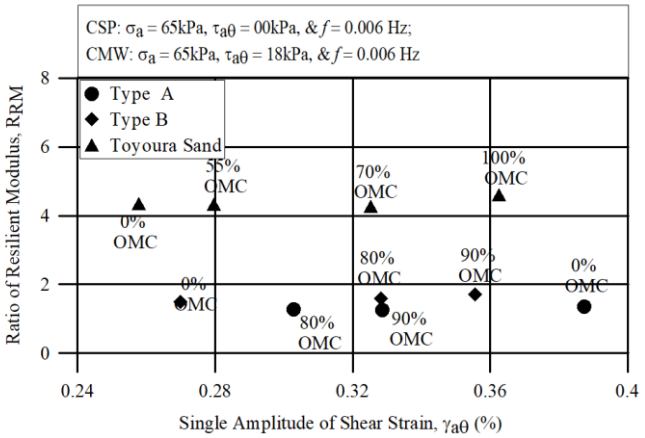

Figure 17 Effects of shear strain on ratio of resilient modulus

The effects of the single amplitude of shear strain on the resilient modulus increase with decreasing fine percentage as shown in Figure 17, where Toyoura sand has the highest dependency towards the PSAR. The relationships between the ratio of moisture content – single amplitude of shear strain – the ratio of resilient modulus of non-expansive soils however seem to behave linear relations, while expansive soil follows a similar trend excluding air-dried specimens. The summary of Figures 15 to 17 further indicates that the ratios of resilient modulus of fine-grain materials have a range of 1.5 to 1.8, while coarse-grain materials are at 4.5 to 5 range.

5. CONCLUSIONS

In this study, three types of materials including one expansive soil were prepared at different moisture contents and subjected to two types of cyclic loading conditions by replicating the cyclic triaxial and moving load tests. The findings of the study can be summarised as follows:

1) The cumulative resilient deformation of any soil type at any saturation level increases with the number of loading cycles and the rate of accumulation rate decreases with increasing in the number of loading cycles.
2) The presence of the PSAR reduces the resilient modulus compared to the cyclic single-point loading tests irrespective of the soil type and saturation level.
3) At the design stage, when the foundation modulus is obtained from cyclic single-point loading conditions, the track designer should reduce the resilient modulus to account for the PSAR effects.
4) For fine-grain materials, this reduction factor (i.e. ratio of the resilient modulus) can be used as 1.5 to 2 and it is a range of 4 to 5 for coarse-grain materials.
5) The degree of saturation gradually decreases the resilient modulus irrespective of the loading method (i.e. with or without PSAR) and soil type. The use of optimum moisture content seems to be a conservative approach in estimating the resilient modulus.
6) However, at a higher saturation level, the designer has to use the upper margin of the ratio of resilient modulus to account for the effects of the PSAR on the results of cyclic single-point loading conditions.

6. REFERENCES

ASTM D1557 – 12e1 (2012) "Standard test methods for laboratory compaction characteristics of soil using modified effort (56,000 ft-lbf/ft^3 (2,700 kN-m/m^3))", ASTM International.

ASTM D6913/D6913M-17 (2017) "Standard test methods for particle-size distribution (gradation) of soils using sieve analysis", ASTM International.

ASTM D7928-17 (2017) "Standard test methods for particle-size distribution (gradation) of soils using the sedimentation (hydrometer)", ASTM International.

Bishop, A. W. (1959) "The principal of effective stress", Teknisk Ukeblad, 106, Issues 39, pp895-863.

Burrow, M. P. N., Bowness, D., and Ghataora, G. S., (2007). "A comparison of railway track foundation design methods", Proceedings of the Institution of Mechanical Engineers, Part F: Journal of Rail and Rapid Transit, 221, Issues 1, pp1-12.

Cai, Y., Wu, T., Guo, L., and Wang, J. (2018). "Stiffness degradation and plastic strain accumulation of clay under cyclic load with principal stress rotation and deviatoric stress variation", Journal of Geotechnical and Geoenvironmental Engineering, 144, Issue 5.

Dareeju, B., Gallage, C., and Dhanasekar, M., (2014) "A comparative analysis of the conservative bridge transition design approaches", Proceedings of the Conference on Railway Excellence: Rail Transportation for Vital Economy, Australia, pp649-657.

Dareeju, B., Gallage, C., Ishikawa, T., and Dhanasekar, M., (2017) "Effects pf principal stress axis rotation on cyclic deformation characterisitcs of rail track subgrade materials", Soils and Foundations, 57, Issues 3, pp423-438.

Gallage, C., Dareeju, B., and Dhanasekar, M., (2013) "State-of-the-art: track degradation at bridge transitions", Proceedings of 4th Int. Conference on Structural Engineering and Construction Management, Sri Lanka, pp40-52.

Gräbe, P. J., and Clayton, C. R. I., (2009) "Effects of principal stress rotation on permanent deformation in rail track foundation", Journal of Geotechnical and Geoenvironmental Engineering, 4, pp555-565.

Gräbe, P. J., and Clayton, C. R. I., (2014) "Effects of principal stress rotation on resilient behaviour in rail track foundation", Journal of Geotechnical and Geoenvironmental Engineering, 140, Issues 2.

Gräbe, P. J., Shaw, F. J., and Clayton, C. R. I., (2005) "Deformation measurement on a heavy haul track formation", Proceeding of 8th Int. Heavy Haul Conference, VA, pp667-692.

Han, Z., and Vanapalli, S. K., (2016), "State-of-the-art: prediction of resilient modulus of unsaturated subgrade soils", International Journal of Geotechnics, 16, Issue 4.

Hibbitt, K and Sorensen, I (2005) "ABAQUS/Explicit user's manuals", Version 6.6: Pawtucket.

Hirakawa, D., Kawasali, H., Tatsuoka, F., and Momoya, Y. (2002) "Effects of loading conditions on the behaviour of railway track in the laboratory model tests", Proceedings of 6th Int. Conference on the Bearing Capacity of Roads, Railway and Airfields, Portugal, pp1295-1305.

Inam, A., Ishikawa, T, and Miura, S., (2012) "Effect of principal stress axis rotation on cyclic plastic deformation characteristics of unsaturated base course material", Soils and Foundations, 52, Issues 3, pp465-480.

Indraratna, B., Sun, Q., No, N. T., and Rujikiatkamjorn, C. (2017) "Current research into ballasted rail tracks: model tests and their practical implications", Australian Journal of Structural Engineering, 18, Issue 3, pp204-220.

Ishikawa, T., and Miura, S., (2015) "Influence of moving wheel loads on mechanical behavaior of submerged granular roadbed", Soils and Foundations, 55, Issues 2, pp242-257.

Ishikawa, T., Sekine, E., and Miura, S., (2011) "Cyclic deformation of granular materials subjected to moving-wheel loads", Canadian Geotechnical Journal, 48, Issues 5, pp691-703.

Kodikara, J. (2012) "New framework for volumetric constitutive behaviour of compacted unsaturated soils", Canadian Geotechnical Journal, 49, Issues 1, pp1227-1243.

Lekarp, F., Isacsson, U., and Dawson, A. R. (2000) "State of the art I: Resilient response of unbound aggregates", Journal of Transportation Engineering, 126, Issues 1, pp66-75.

Li, D., Sussmann, T., Hyslip, J., and Chrismer, S. (2015). Railway geotechnics: Taylor & Francis Ltd.

Momoya, Y., (2004) "A study on deformation characteristics of railway roadbed considering an effect of moving wheel loading", PhD thesis, Railway Technical Research Institute, Japan. [in Japanese].

Momoya, Y., Sekine, E., and Tatsuoka, F., (2005) "Deformation characteristics of railway roadbed and subgrade under moving-wheel load", Soils and Foundations, 45, Issues 4, pp99-118.

O'Riordan, N. and Phear, A. (2001) "Design and construction control of ballasted track formation and subgrade for high speed lines", Proceedings of Int. Conference of Railway Engineering, UK.

Rajeev, P., Chan, D., and Kodikara, J., (2012) "Ground-atmosphere interation modelling for long-term prediction of soil moisture and temperature", Canadian Geotechnical Journal, 49, Issues 9, pp1059-1073.

Salour, F., Erlingsson, S., and Zapata, C., (2014). "Modelling resilient modulus seasonal variation of silty sand subgrade soils with matric suction control", Canadian Geotechnical Journal, 51, Issue 12, pp1413-1422.

Sayeed, M. A. (2016) "Design of ballast railway track foundation using numerical modelling with special reference to high speed trains", PhD thesis, Curtin University, Australia.

Sun, Q. D., Indraratna, B., and Nimbalkar, S. (2015) "Effect of cyclic loading frequency on the permanent deformation and degradation of railway ballast", Geotechnique, 64, issue 9, pp746-751.

Yang, L. A., Powrie, W., and Priest, J. A. (2009) "Dynamic stress analysis of a ballasted railway track bed during train passages", Journal of Geotechnical and Geoenvironmental Engineering, 135, Issues 5, pp 680-689.